Effect of Cobalt Addition on Thermal Cycling Behaviour of $Ti_{50}Ni_{(50-x)}Co_x$ Shape Memory Alloys

G. Swaminathan[1], V. Sampath[2, *], S. Santosh[3]

[1]Department of Mechanical Engineering, PSG Institute of Technology and Applied Research, Neelambur, Coimbatore - 641 062, India.

[2]Department of Metallurgical and Materials Engineering, Indian Institute of Technology Madras, Chennai 600 036, India.

[3]Department of Mechanical Engineering, Sri Sivasubramaniya Nadar College of Engineering, Kalavakkam - 603 110, India.

*Corresponding author: vsampath@iitm.ac.in

Abstract

The effect of adding Co on the temperature cycling behaviour of ternary $Ti_{50}Ni_{(50-x)}Co_x$ (x=1,2,3) alloys was experimentally studied in this work. The alloys were prepared using a vacuum induction furnace, followed by subjecting them to homogenization, hot-rolling and annealing processes. The alloys were subjected to thermal cycling experiments in a nitrogen atmosphere by differential scanning calorimetry under stress-free conditions between their transformation temperatures. The results indicate that adding Co to NiTi alloys decreases their transition temperatures, improves the thermal cycling stability apart from suppressing the R-phase formation on cooling during cycling. The changes are due to the addition of Co introducing solid solution strengthening and generation of dislocations during cyclic phase transformations, as confirmed by the hardness test results and TEM micrographs, respectively.

Keywords: NiTiCo SMAs; Transition temperatures; Differential scanning calorimetry; Thermal cycling.

1. Introduction

Phase transitions occur in shape memory alloys (SMAs) on heating (martensite → austenite) and cooling (austenite → martensite), and the phases are crystallographically reversible and enable them to memorize their high-temperature

shape [1–3]. Based on the transformation temperatures, SMAs are divided into low-temperature (A_s< 0 °C) and high-temperature (A_s > 100°C) shape memory alloys, where A_s, A_f, M_s and M_f indicate austenite start, austenite finish, martensite start and martensite finish, respectively [4].

Commercially, NiTi-based alloys are considered to be one of the most successful among SMAs and are therefore used in many engineering (actuators, robotic arm grippers and pipe couplings) and medical (stents and orthodontic archwires) applications because of their appreciable mechanical properties and superior biocompatibility, respectively [5–7]. Moreover, the shape memory properties, i.e., transition temperatures, recovery strain and thermal hysteresis, of the binary SMAs are modified/tailored by adding ternary or quaternary elements to them [1,8,9]. During substitution for Ni and Ti in the ordered parent B2/B19' crystal structure, local atomic bonds expand or contract depending on the intrinsic properties of the ternary/quaternary element, including crystal structure, atomic radius, electronegativity, and valency [10].

The shape memory alloys that are intended for CryoFit couplings (a tradename for a shape memory alloy-based coupling) [11] and tube fittings [12] are so designed that their transition temperatures are much lower than room temperature, i.e., low-temperature shape memory alloys. By replacing Ni atoms with Co [13], Cr [10], Fe [14], or Nb [15,16] atoms, the transition temperatures of NiTi alloys can be substantially lowered. In NiTiFe shape memory alloys that are meant for cryofit applications, the transition temperatures are lowered by adding Fe to binary Ni-Ti SMAs. In contrast, the corrosion resistance of these alloys is impaired due to iron addition. In this context, NiTiCo alloys are more appropriate for this kind of application as adding Co does not in any way impair the corrosion behaviour of the binary NiTi SMAs [17–19].

The phase transformation of NiTiCo alloys involves austenite-to-martensite transition on cooling through a single-step or a double-step transformation (involving the formation of R-phase) [1,20,21]. Not only does Co addition decrease the transformation temperatures, but also, on the other hand, increases the work hardening

coefficient and yield stress of binary NiTi SMAs [22]. Moreover, ternary NiTiCo SMAs show improved mechanical and fracture behaviour on subjecting them to aging and cold deformation [23]. Unlike binary NiTi alloys, ternary NiTiCo (≤ 2 at.% of Co) alloys show a higher loading/unloading plateau (up to 30%) and a higher modulus [24]. NiTiCo SMAs exhibit fatigue properties similar to binary NiTi alloys under high-cycle and medium-cycle conditions. Moreover, the aging treatment helps raise the transition temperatures of the NiTiCo alloys due to the change in composition of the matrix due to the promotion of precipitate particles, i.e., Ni/Co-rich phases [25]. The ternary NiTiCo SMAs, as compared to binary NiTi SMAs, exhibit higher stress at comparable strain levels, making it possible to fabricate devices with thinner section thicknesses and smaller diameters with comparable or improved functional performances [19].

In pipe coupling applications, the alloy is cooled below its M_f temperature before being deformed by a mandrel. Subsequently, it is inserted into the room-temperature connecting tubes [26,27]. The temperature difference between the coupler and the pipe causes the martensite to revert to austenite. As a result, the coupler firmly holds the tubes. These applications require frequent fitting and removal of the coupler for repair and maintenance purposes. Generally, the pipe couplers are expected to have a fatigue life span of at least ten cycles [28]. As the alloy is highly deformable in the martensitic state, the coupler is often removed by cooling it below M_f temperature. This frequent fitting and removal of the coupler makes the material to undergo thermal cycling. Consequently, these alloys are prone to thermal cycling fatigue.

When SMAs are exposed to thermal, mechanical, or thermomechanical cycling, their shape memory properties, i.e., transformation temperatures, recovery strain and thermal hysteresis, are affected. The variation in the functional properties introduced by the occurrence of the intermediate R-phase transformation upon cooling and the increased number of cycles can adversely affect the performance of SMA-based components/devices. As mentioned earlier, the addition of Co to NiTi (NiTiCo SMA) could be one of the potential candidate materials for cryofit applications. However, the effect of cyclic phase transformation on the transformation behaviour of NiTiCo

SMAs has not been studied yet. In our work, therefore, the role of Co introduction, up to 3 at.%, on thermal cycling behaviour, such as the modification of transition temperatures and thermal cycling stability, of NiTiCo alloys were experimentally investigated, and the results are presented in detail.

2. Materials and Methods

The materials for the study, namely $TiNi_{50-x}Co_x$ (x=1,2,3) alloys, were melted and solidified in a graphite crucible using a vacuum induction melting furnace. The NiTiCo alloy compositions are given in The X-ray diffraction technique was employed to conduct phase analysis on the annealed samples using a Bruker D8 Discover model XRD equipment. The machine operated at a voltage of 40 kW, a current of 30 mA, and utilised Cu-Kα1 radiation with a wavelength of 1.5406 Å. The range of 2θ was from 10° to 90° and the step-size was 0.02° with the time taken for each step is 1s.

Table 1. The alloy discs were subsequently solutionized at 900 ℃ for 3 h in an Ar-filled quartz tube, following which they were quenched into water maintained at the ambient temperature. The specimens were then rolled down from 3 mm to 1 mm in multiple passes with gradual reduction of thickness at 900 ℃ in open air condition. The sheet samples were annealed at 900 ℃ for 30 min in an Ar-filled quartz tube, and then they were quenched into water at room temperature. The X-ray diffraction technique was employed to conduct phase analysis on the annealed samples using a Bruker D8 Discover model XRD equipment. The machine operated at a voltage of 40 kW, a current of 30 mA, and utilised Cu-Kα1 radiation with a wavelength of 1.5406 Å. The range of 2θ was from 10° to 90° and the step-size was 0.02° with the time taken for each step is 1s.

Table 1 Nominal compositions of NiTiCo SMAs used in this study.

Sl. No.	Nomenclature	Composition of the alloy (at. %)
1.	NTCo1	$Ti_{50}Ni_{49}Co_1$
2.	NTCo2	$Ti_{50}Ni_{48}Co_2$

3.	NTCo3	$Ti_{50}Ni_{47}Co_3$

The test samples were prepared from the annealed alloys for thermal cycling experiments, to be conducted using a Discovery 25 model DSC under an N_2 atmosphere for 20 cycles under stress-free conditions. The cycling temperature range (50 to -140 ℃) was chosen based on the alloy's transformation temperatures with the rate of heating and cooling at 20 ℃/min. Hardness tests were performed on each sample using an Innovatest Falcon 603 model hardness tester. Seven indentations were made on each sample by applying a force of 100 kgf for a dwell time of 10 s. The microstructural examination was done using a Tecnai 20 model TEM operated at a voltage of 200 kV in the bright field imaging mode. The specimens for the TEM studies were first mechanically thinned down from 1 mm to 80 μm using emery sheets, followed by disc punching and electropolishing. The composition of the electrolyte used to prepare the TEM samples was 15% H_2SO_4 and 85% methanol (vol.%). The operating conditions for the electropolishing were: potential = 15V; temperature = -30℃.

3. Results

The X-ray diffractograms obtained for the phase analysis are given in Fig. 1. The room temperature X-ray diffractograms reveal that all the alloys, i.e., NiTiCo1, NiTiCo2 and NiTiCo3, show the presence of austenite (B2 phase), implying that the martensite transformation temperatures (M_s and M_f) are below room temperature. Similarly, the DSC thermogram, as shown in Fig. 2, corresponding to these alloys, shows that adding Co to NiTi causes a reduction in the transition temperatures and is, therefore, aptly called low-temperature shape memory alloys [4]. Moreover, from the DSC thermograms (Fig. 2), it is seen that austenite transforms to martensite in two stages, i.e., first to R-phase (A→R) and subsequently, to martensite (R→M), upon cooling. However, the reverse transition (M→A) upon heating involves only one-step.

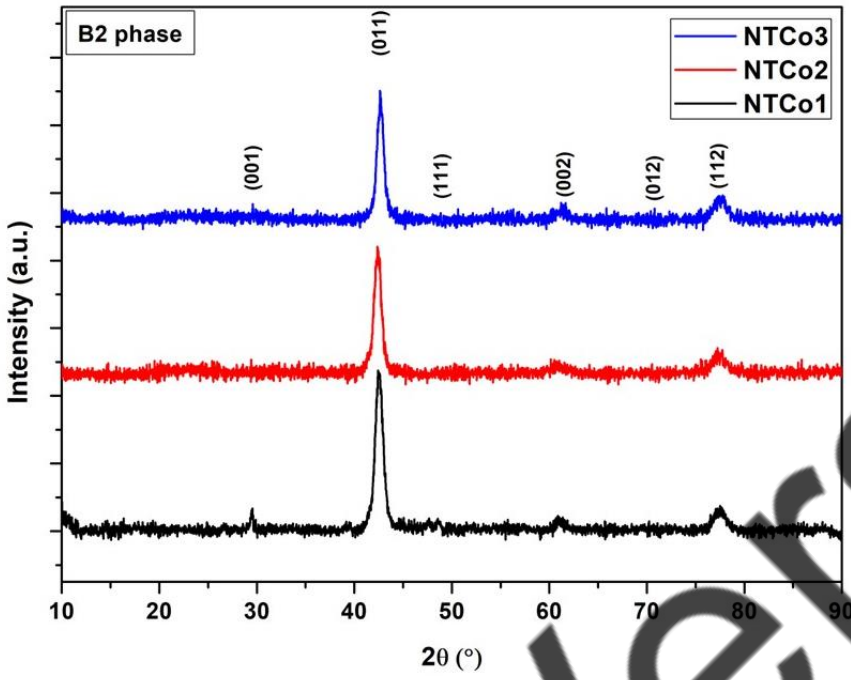

Fig. 1 XRD diffractograms for NiTiCo shape memory alloys

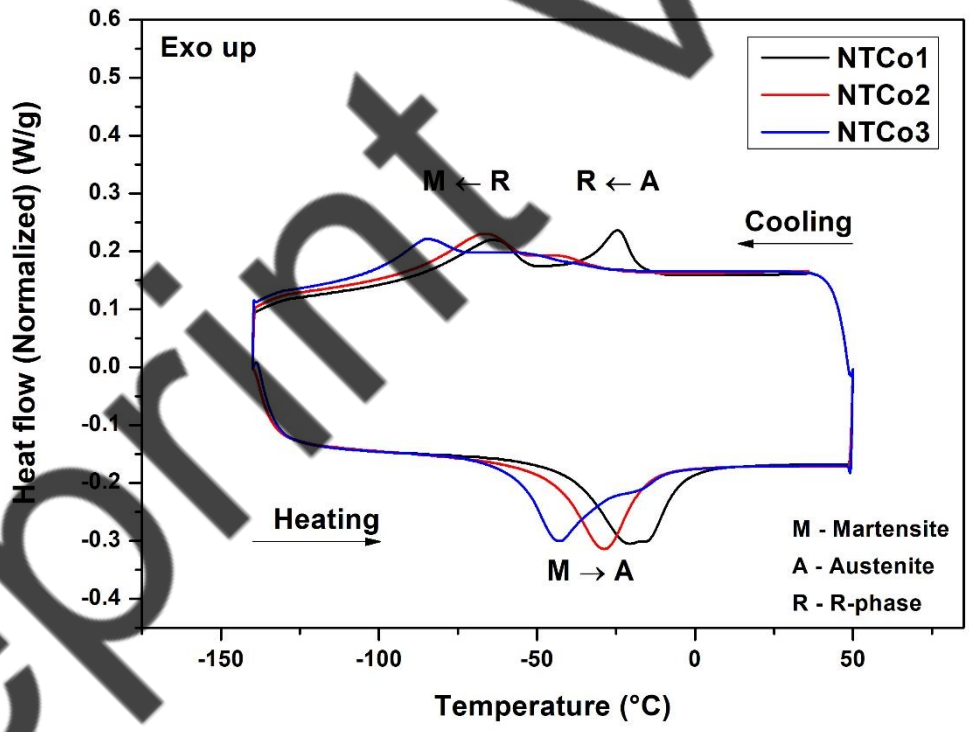

Fig. 2 DSC thermogram for NiTiCo SMAs before thermal cycling

The NTCo1 alloy on cooling exhibits a twin-step transition, and a mono-step transition upon heating, as given in Fig. 3 (a). As Fig. 4 (a) reveals, thermal cycling causes the austenite-martensite transition temperatures to reduce with the increasing

number of cycles. Interestingly, upon cooling of austenite to form R-phase (A→R), the alloy shows stable transformation behaviour, unlike the martensite to R-phase transition (R→M). During the initial cycles, the martensite and austenite transition temperatures undergo a smaller reduction and then saturate.

The addition of 2 at. % of Co to NiTi further decreases the alloy's martensite and R-phase transition temperatures. From Fig. 3 (b), it is observed that the temperature difference between the R-phase and martensite has significantly reduced, and the addition of Co has also reduced the peaks corresponding to the R-phase transition. Moreover, the decrease in the M_s and M_f temperatures of the NTCo2 alloy is lower in comparison with the NTCo1 alloy, as illustrated in Fig. 4 (b).

Similarly, the addition of 3 at. % of Co to NiTi decreases the transition temperatures further, as indicated in Fig. 3 (c). However, the variation in the transition temperatures caused by increased number of cycles is much lower, as indicated in Fig. 4 (c), in comparison with the NTCo1 and NTCo2 SMAs. Moreover, the NTCo3 alloy shows the suppressed R-phase during cooling, as depicted in Fig. 3 (c). It implies that the inclusion of Co suppresses the R-phase and promotes the formation of the martensite phase directly from austenite while cooling. As observed in Fig. 3 (a-c), the variation in the A_s and A_f temperatures is lesser in comparison to the M_s and M_f temperatures. This result implies that thermal cycling significantly affects the formation of martensite from austenite than the formation of austenite from martensite. Moreover, the addition of Co stabilizes the alloy against the decreased transition temperatures with increased number of cycles, as shown in Fig. 4 (c).

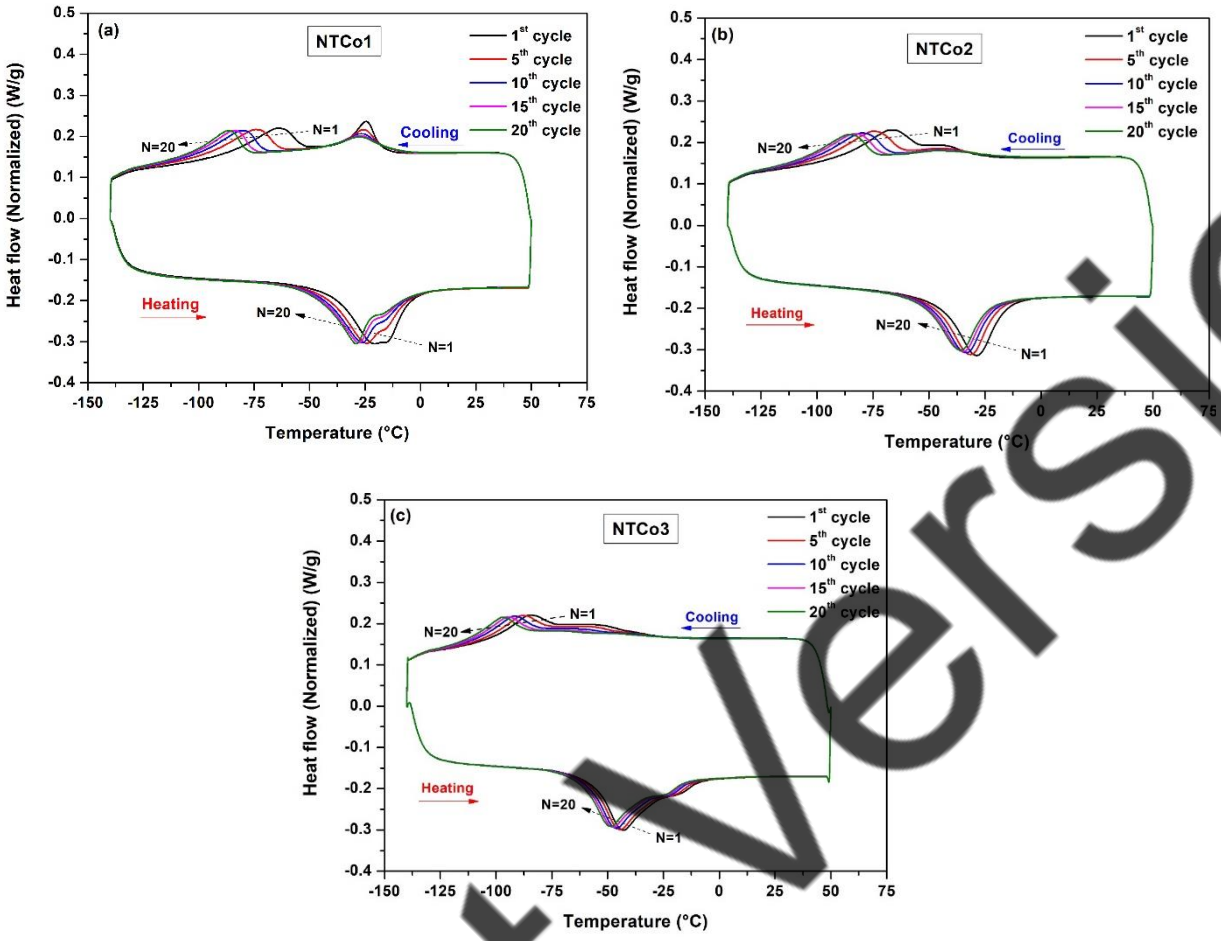

Fig. 3 DSC thermogram showing thermal cycling characteristics of SMAs: (a) NiTiCo1, (b) NiTiCo2 and (c) NiTiCo3.

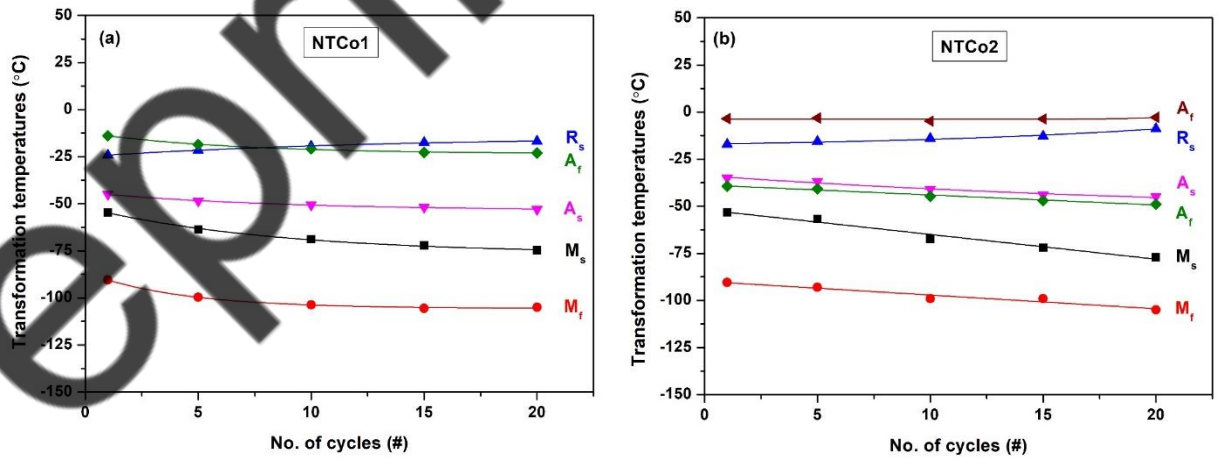

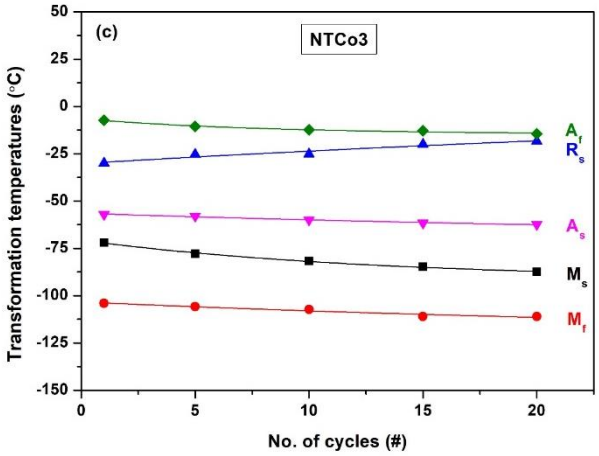

Fig. 4 Influence of thermal cycling on transformation temperatures of (a) NiTiCo1, (b) NiTiCo2 and (c) NiTiCo3 SMAs

In a shape memory alloy, the width of thermal hysteresis is an indication of the ease with which the austenite-to-martensite transition (A→M) and the martensite-to-austenite transition (M→A) occurs. It can be directly obtained from the transformation temperatures of an SMA, since it is a measure of the temperature difference between A_f and M_s, i.e., A_f-M_s [29,30]. However, the occurrence of an intermediate R-phase poses the problem of convolution of peaks corresponding to R-phase and martensite phase. Therefore, in the present work, the difference between A_p (austenite peak) and M_p (martensite peak) was used to calculate the thermal hysteresis width [31,32]. A larger hysteresis width indicates a higher energy dissipation during the transformation [33]. The hysteresis width of an SMA is dictated by the geometric compatibility of the transforming phases [34]. From Fig. 5, it can be seen that the addition of Co to NiTi decreases the thermal hysteresis width and then increases slightly before cycling. In addition, irrespective of the amount of Co added, with increased number of thermal cycles the hysteresis width increases, as indicated in Fig. 6. However, formation and suppression of the intermediate R-phase with increased number of cycles affect the rate at which the changes occur.

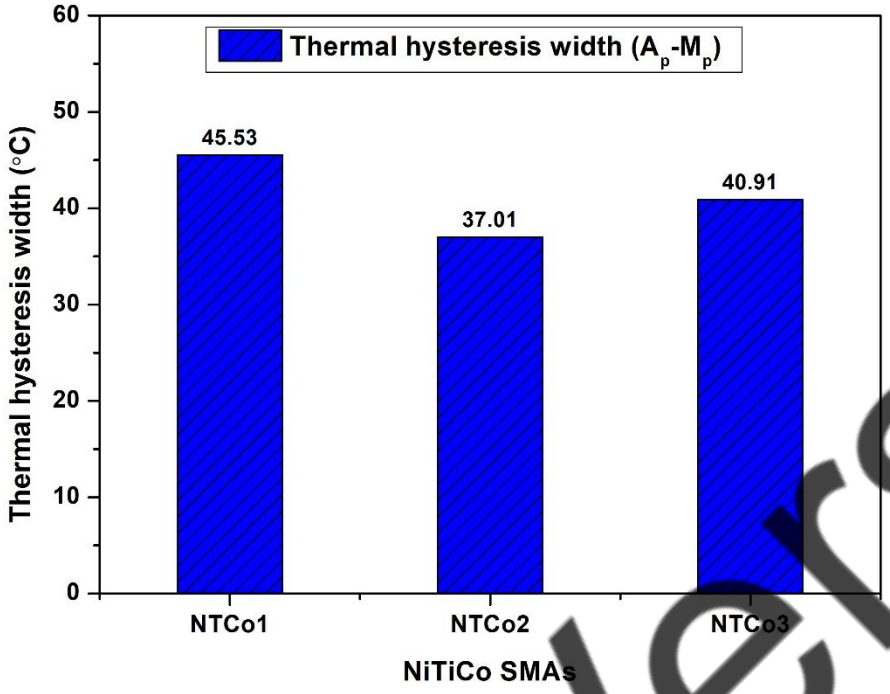

Fig. 5 Histogram comparing the thermal hysteresis width (A_p - M_p) of NiTiCo SMAs with different Co contents before thermal cycling.

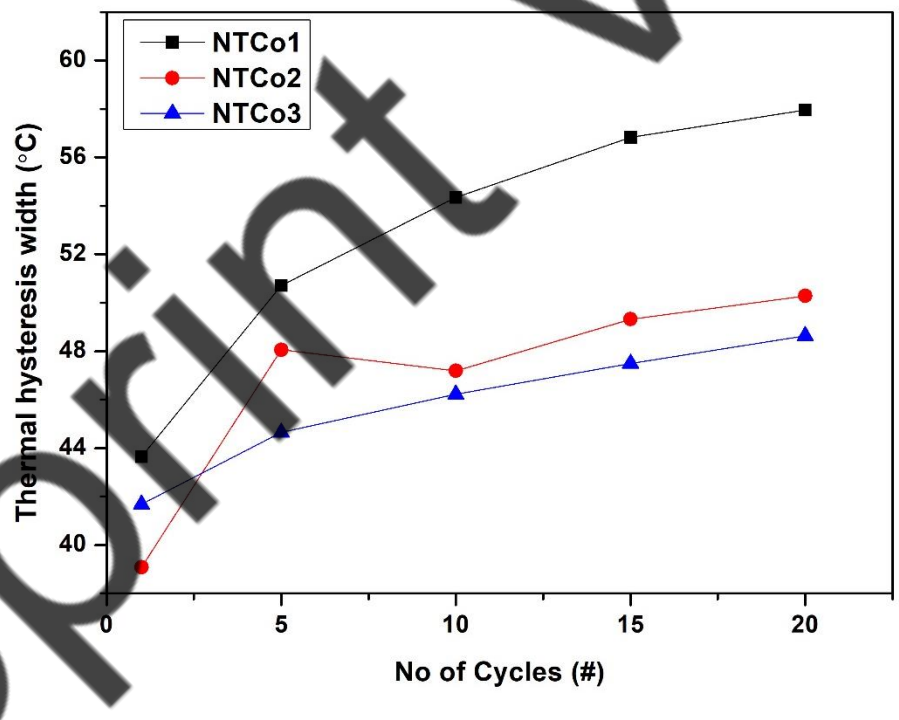

Fig. 6 Effect of thermal cycling on thermal hysteresis width of NiTiCo SMAs

4. Discussions

The observed effects, i.e., reduced transition temperatures and variations in the thermal hysteresis width, are caused by the solid solution strengthening of NiTi alloy by the Co addition and the creation of lattice defects, i.e., dislocations, upon thermal

cycling [10]. When the Co atoms substitute for Ni atoms in NiTi alloy, the solution strengthening of the alloy occurs due to the strain field effect caused by the distortion of crystal lattice due to the size mismatch between Co (200 pm) and Ni (163 pm) atoms. These strain fields hinder the motion of the martensitic plates during cooling, and thereby necessitating additional driving force, i.e., undercooling, to transform from austenite to martensite [28,35]. This leads to reduced transition temperatures. The extent of Co addition to the alloy influences the degree of distortion of the crystal lattice.

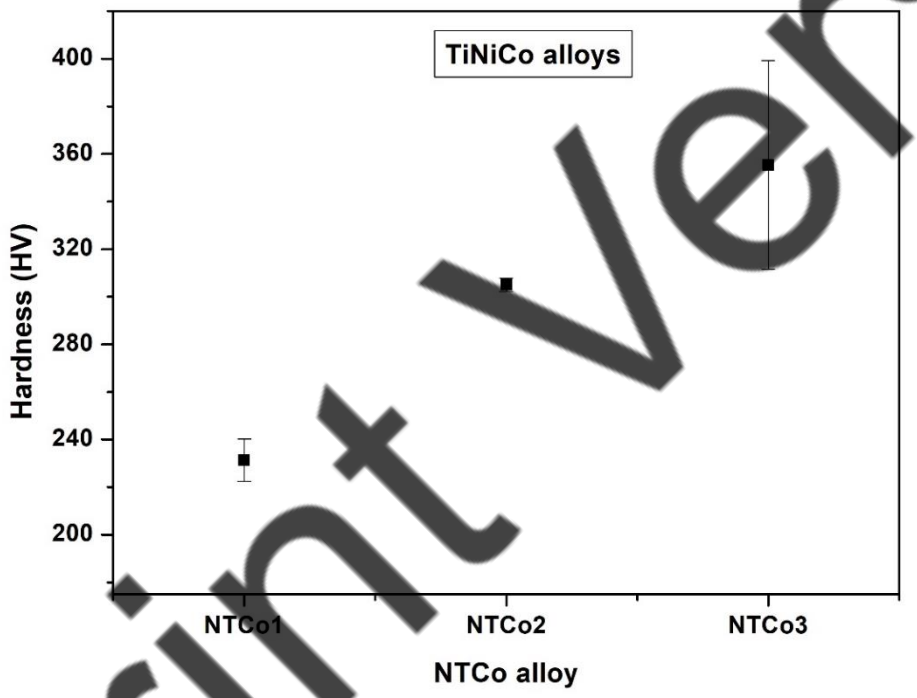

Fig. 7 Hardness of NiTiCo SMAs

When the Co content is increased, the strength of the alloy increases. This indicates that the distortion of the crystal lattice increases with increased Co addition. Therefore, the resistance for the forward transformation (A→M) increases with increasing Co content, thereby causing a decrease in transition temperatures, as shown in Fig. 2. This observation is supported by the hardness tests conducted on the NiTiCo SMAs. Generally, an increase in the hardness of an alloy indicates increased strengthening of the alloy. Referring to Fig. 7, the hardness of the alloy rises with a raise in Co content. The hardness results are consistent with the observed reduction in transformation temperatures.

The effect of thermal cycling, i.e., reduction in transition temperatures with increased number of cycles, is caused by the generation of dislocations [36]. During austenite to martensite phase transformation, the dislocations, also known as transformation-induced dislocations, are generated so as to accommodate the strain arising from the incompatibility of the transforming phases [37,38]. It is a well-known fact that the dislocations hinder the mobility of the martensitic plates to grow. As a result, the transformation temperatures decrease [39]. The presence of dislocations in the alloys, i.e., (a) NiTiCo1, (b) NiTiCo2 and (c) NiTiCo3, after thermal cycling can be seen in their TEM micrographs, as illustrated in Fig. 8.

Moreover, the creation and multiplication of dislocations harden the alloys further due to strain hardening effect, and thus reaches a point beyond which further generation becomes difficult. As a result, the rate of dislocation generation in the alloys is higher during the initial stages of cycling, and, subsequently, tends to saturate. This trend is attested by the changes in the transformation temperatures profiles (Fig. 4). Also, the nucleation of the martensite phase is affected by the density of dislocations, so that high values of this density can strengthen the matrix, hindering the shear mechanism of the martensitic transformation and, therefore, requiring a greater degree of supercooling to complete the phase transformation of the martensite, which causes a reduction in the M_s temperature values [40].

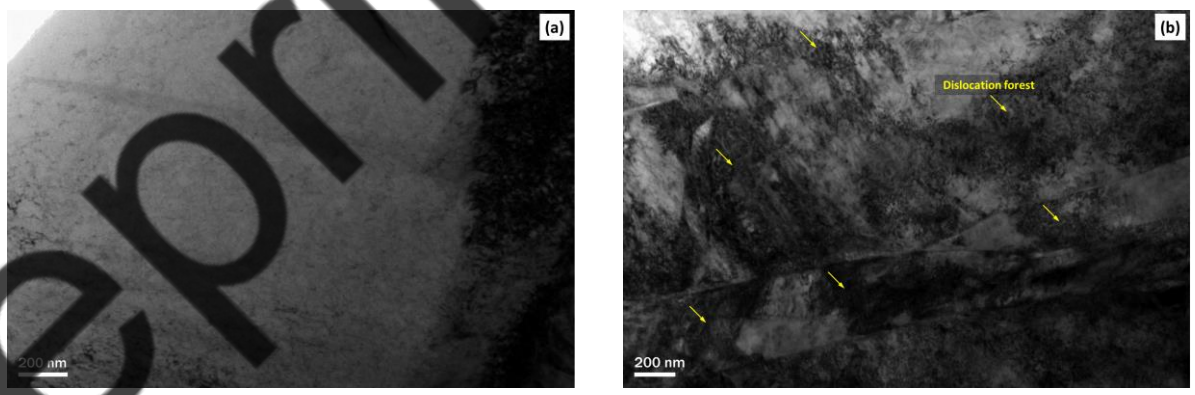

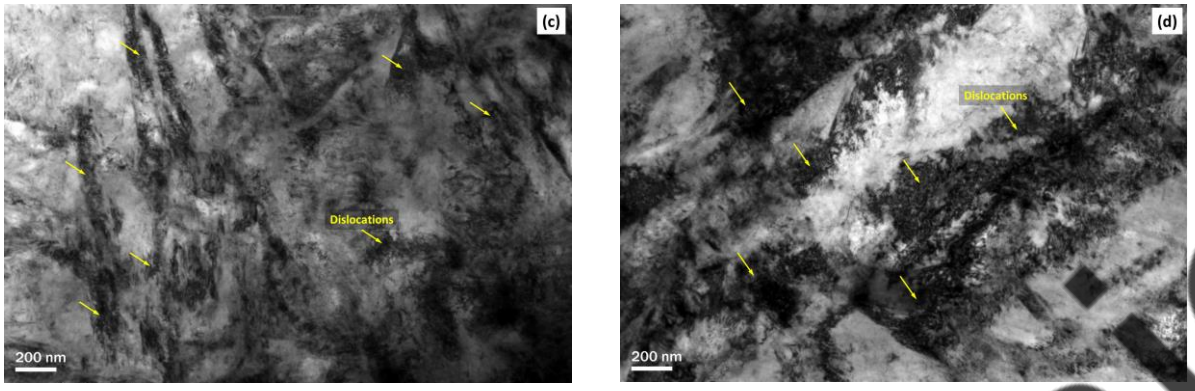

Fig. 8 TEM micrographs of NiTiCo SMAs: (a) NiTiCo1 before thermal cycling and (b) NiTiCo1, (c) NiTiCo2 and (d) NiTiCo3, showing dislocation sub-structure introduced after thermal cycling

However, the shift in the transformation temperatures is smaller in NiTiCo3 as compared to the NiTiCo3 SMA. These results indicate that the increase in Co content increases the stability of the phase transition, i.e., smaller changes in the transformation temperatures, as shown in Fig. 9. This is caused by the increased strength of the alloy, i.e., increase in modulus of elasticity, due to the effect of both solution strengthening (alloying addition) and strain hardening (generation of dislocations). Generally, the strengthening of the alloy is considered as an effective strategy to improve the thermal cycling fatigue resistance of SMAs [41]. Moreover, it is observed from Fig. 3 that suppression of R-phase occurs with increasing number of cycles.

Increasing Co addition causes an increase in the Gibbs free energy for the austenite to R-phase transition, thereby suppressing the formation of the R-phase [42]. Consequently, the alloy tends to transform directly to martensite from austenite on cooling instead of undergoing a double-step transition, i.e., A→R transformation, followed by R→M transformation. Moreover, it is noted from Fig. 4 (a-c) that there is no variation in the R_s temperature as the number of thermal cycles increases. This observation suggests that the change in the density of dislocation with increased number of thermal cycles does not affect the R-phase transformation temperatures. The R_s and R_f temperatures are less sensitive to thermal cycles than martensitic

transformation because it experiences much smaller lattice distortions, with the maximum strain being ~1% [43].

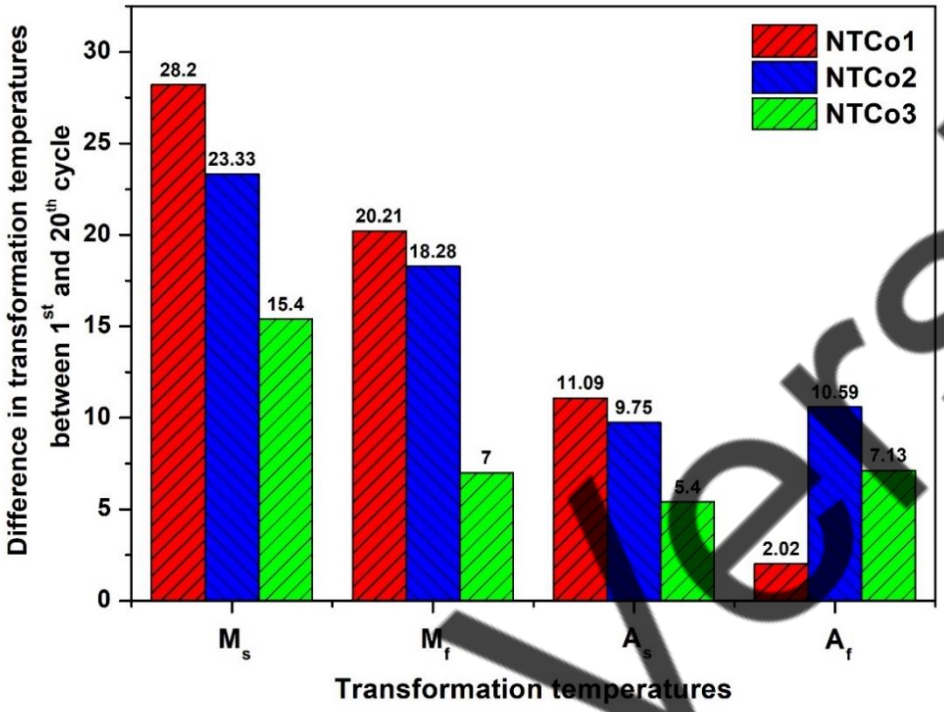

Fig. 9 Histogram comparing the stability of transformation temperatures of NiTiCo SMAs with different Co contents.

The presence of high dislocation density resists the martensite transformation (lattice distortion) during cooling. The transformations with large lattice distortion, such as austenite-to-martensite transformation, have a much larger resistance. In contrast, transformations with smaller lattice distortions, such as the austenite-to-R-phase transition, have a less significant effect [44]. However, the R_s and R_f temperatures of the alloy are highly influenced by the Co content of the NiTi matrix and the Ti:Ni ratio of the alloy.

Recent work has reported similar observations for Ni-rich Ni-Ti SMAs [45]. This observation has a practical significance considering their applications, as the stability of the couplings and pipe fittings are primarily dependent on the phases present. When a coupler undergoes R-phase transformation upon cooling and heating, the strain involved in the transformation is restricted to less than 1%. As a result, it becomes

difficult to deform the material at lower temperatures and thereby posing difficulty during the pipe fitting process.

5. Summary and Conclusions

The effect of Co addition on thermal cycling fatigue behaviour of $Ti_{50}Ni_{50-x}Co_x$ SMAs was studied. The alloys were subjected to cyclic phase transformation between their transformation temperatures, and the variation in their shape memory characteristics and cyclic stability were analysed. The results reveal that Co addition introduces a solid solution strengthening effect on NiTi alloy and thereby decrease its transition temperatures. Moreover, increasing the Co content of the alloy leads to the suppression of the R-phase upon cooling, thereby increasing the thermal cycling stability of NiTiCo SMAs. These observations are attributed to the changes in elastic modulus caused by solid solution strengthening apart from the introduction of local elastic strain brought about by the creation of lattice defects, i.e., dislocations, upon thermal cycling. Based on the current study, it is, therefore, proposed that the NiTiCo3 SMA is suitable for coupling and pipe fitting applications.

CRediT authorship contribution statement

G. Swaminathan - Conceptualization, Methodology, Testing, Characterization, Validation, Formal analysis, Investigation, Writing – original draft. **V. Sampath** - Supervision, Project administration, Formal analysis, Resources, Writing – review & editing. **S. Santosh** – Alloy preparation, Secondary processes, and Methodology.

Declaration of competing interest

The authors declare that they have no known competing financial or personal interests that could have appeared to influence the work reported in this article.

Data availability statement

The data will be made available upon reasonable request.

Acknowledgement

The authors would like to acknowledge the Science and Engineering Research Board, Department of Science Technology, India, for the financial support under grant number CRG/2019/002267.

References

[1] Otsuka K and Ren X 2005 Physical metallurgy of Ti-Ni-based shape memory alloys *Prog. Mater. Sci.* 50 511–678

[2] Bhattacharya K, Conti S, Zanzotto G and Zimmer J 2004 Crystal symmetry and the reversibility of martensitic transformations *Nature* 428 55–9

[3] Kumar P K and Lagoudas D C 2008 Introduction to shape memory alloys *Shape memory alloys* (Springer) pp 1–51

[4] Benafan O, Bigelow G S, Garg A and Noebe R D 2019 Viable low temperature shape memory alloys based on Ni-Ti-Hf formulations *Scr. Mater.* 164 115–20

[5] Van Humbeeck J 2001 Shape memory alloys: a material and a technology *Adv. Eng. Mater.* 3 837–50

[6] Predki W, Knopik A and Bauer B 2008 Engineering applications of NiTi shape memory alloys *Mater. Sci. Eng. A* 481–482 598–601

[7] Hodgson D E, Ming W H and Biermann R J 1990 Shape memory alloys *ASM Int. Met. Handbook, Tenth Ed.* 2 897–902

[8] Frenzel J, Wieczorek A, Opahle I, Maaß B, Drautz R and Eggeler G 2015 On the effect of alloy composition on martensite start temperatures and latent heats in Ni-Ti-based shape memory alloys *Acta Mater.* 90 213–31

[9] Shao L, Zhao Y, Jiménez A, Vázquez M and Zhang Y 2017 Shape Memory and Huge Superelasticity in Ni--Mn--Ga Glass-Coated Fibers *Coatings* 7 5

[10] Xue D, Xue D, Yuan R, Zhou Y, Balachandran P V., Ding X, Sun J and Lookman T 2017 An informatics approach to transformation temperatures of NiTi-based shape memory alloys *Acta Mater.* 125 532–41

[11] Mohd Jani J, Leary M, Subic A and Gibson M A 2014 A review of shape

memory alloy research, applications and opportunities *Mater. Des.* 56 1078–113

[12] Tabesh M, Boyd J, Atli K C, Karaman I and Lagoudas D 2018 Design, fabrication, and testing of a multiple-actuation shape memory alloy pipe coupler *J. Intell. Mater. Syst. Struct.* 29 1165–82

[13] Santosh S and Sampath V 2019 Effect of Ternary Addition of Cobalt on Shape Memory Characteristics of Ni-Ti Alloys *Trans. Indian Inst. Met.* 72 1481–4

[14] Zhang Y qiu, Jiang S yong, Zhu X ming, Zhao Y nan, Liang Y long and Sun D 2017 Influence of Fe addition on phase transformation behavior of NiTi shape memory alloy *Trans. Nonferrous Met. Soc. China (English Ed.* 27 1580–7

[15] Qu W T, Gong H, Wang J, Nie Y S and Li Y 2019 Martensitic transformation, shape memory effect and superelasticity of Ti–xZr–(30–x)Nb–4Ta alloys *Rare Met.* 38 965–70

[16] Wei L and Xinqing Z 2009 Mechanical Properties and Transformation Behavior of NiTiNb Shape Memory Alloys *Chinese J. Aeronaut.* 22 540–3

[17] Huang X, Norwich D W and Ehrlinspiel M 2014 Corrosion behavior of Ti-55Ni-1.2Co high stiffness shape memory alloys *J. Mater. Eng. Perform.* 23 2630–4

[18] El-Bagoury N and Khaled K F 2017 Microstructure and corrosion behaviour of NiTiCo shape memory alloys under various aging conditions *Moroccan J. Chem. El- J. Chem. Mor. J. Chem* 5 3–438

[19] Manjeri R M, Norwich D, Sczerzenie F, Huang X, Long M and Ehrlinspiel M 2016 A Study of Thermo-mechanically Processed High Stiffness NiTiCo Shape Memory Alloy *J. Mater. Eng. Perform.* 25 894–900

[20] Bozzolo G, Noebe R D and Mosca H O 2005 Site preference of ternary alloying additions to NiTi: Fe, Pt, Pd, Au, Al, Cu, Zr and Hf *J. Alloys Compd.* 389 80–94

[21] Tatar C and Kurt M 2020 Phase transformation temperatures and physical

characteristics of NiTiCo shape memory alloys produced by arc melting method *Eur. Phys. J. Plus* 135 1–12

[22] Fasching A, Norwich D, Geiser T and Paul G W 2011 An evaluation of a NiTiCo alloy and its suitability for medical device applications *J. Mater. Eng. Perform.* 20 641–5

[23] Kishi Y, Yajima Z and Shimizu K 2002 Relation between tensile deformation behavior and microstructure in a Ti-Ni-Co shape memory alloy *Mater. Trans.* 43 834–9

[24] Singh N, Talapatra A, Junkaew A, Duong T, Gibbons S, Li S, Thawabi H, Olivos E and Arróyave R 2016 Effect of ternary additions to structural properties of NiTi alloys *Comput. Mater. Sci.* 112 347–55

[25] El-Bagoury N 2016 Comparative study on microstructure and martensitic transformation of aged Ni-rich NiTi and NiTiCo shape memory alloys *Met. Mater. Int.* 22 468–73

[26] Niccoli F, Garion C, Maletta C, Sgambitterra E, Furgiuele F and Chiggiato P 2017 Beam-pipe coupling in particle accelerators by shape memory alloy rings *Mater. Des.* 114 603–11

[27] KAUFFMAN G B and MAYO I 1997 The Story of Nitinol: The Serendipitous Discovery of the Memory Metal and Its Applications *Chem. Educ.* 2 1–21

[28] Eggeler G, Hornbogen E, Yawny A, Heckmann A and Wagner M 2004 Structural and functional fatigue of NiTi shape memory alloys *Mater. Sci. Eng. A* 378 24–33

[29] Wang X, Van Humbeeck J, Verlinden B and Kustov S 2016 Thermal cycling induced room temperature aging effect in Ni-rich NiTi shape memory alloy *Scr. Mater.* 113 206–8

[30] Zarnetta R, Takahashi R, Young M L, Savan A, Furuya Y, Thienhaus S, Maaß B, Rahim M, Frenzel J, Brunken H, Chu Y S, Srivastava V, James R D, Takeuchi I, Eggeler G and Ludwig A 2010 Identification of quaternary shape

memory alloys with near-zero thermal hysteresis and unprecedented functional stability *Adv. Funct. Mater.* 20 1917–23

[31] Frenzel J, George E P, Dlouhy A, Somsen C, Wagner M F X and Eggeler G 2010 Influence of Ni on martensitic phase transformations in NiTi shape memory alloys *Acta Mater.* 58 3444–58

[32] Liu Y, Laeng J, Chin T V. and Nam T H 2008 Partial thermal cycling of NiTi *J. Alloys Compd.* 449 144–7

[33] Zhang Z, James R D and Müller S 2009 Energy barriers and hysteresis in martensitic phase transformations *Acta Mater.* 57 4332–52

[34] Cui J, Chu Y S, Famodu O O, Furuya Y, Hattrick-Simpers J, James R D, Ludwig A, Thienhaus S, Wuttig M, Zhang Z and Takeuchi I 2006 Combinatorial search of thermoelastic shape-memory alloys with extremely small hysteresis width *Nat. Mater.* 5 286–90

[35] Lagoudas D C, Miller D A, Rong L and Kumar P K 2009 Thermomechanical fatigue of shape memory alloys *Smart Mater. Struct.* 18 1–12

[36] Miyazaki S, Igo Y and Otsuka K 1986 Effect of thermal cycling on the transformation temperatures of TiNi alloys *Acta Metall.* 34 2045–51

[37] Gu H, Bumke L, Chluba C, Quandt E and James R D 2018 Phase engineering and supercompatibility of shape memory alloys *Mater. Today* 21 265–77

[38] Gao Y, Casalena L, Bowers M L, Noebe R D, Mills M J and Wang Y 2017 An origin of functional fatigue of shape memory alloys *Acta Mater.* 126 389–400

[39] Simon T, Kröger A, Somsen C, Dlouhy A and Eggeler G 2010 On the multiplication of dislocations during martensitic transformations in NiTi shape memory alloys *Acta Mater.* 58 1850–60

[40] Silva D D S, Guedes N G, Oliveira D F, Torquarto R A, Júnior F W, Lima B A S G, Feitosa F R P and Gomes R M 2022 Effects of long-term thermal cycling on martensitic transformation temperatures and thermodynamic parameters of

polycrystalline CuAlBeCr shape memory alloy *J. Therm. Anal. Calorim.* 1–7

[41] Atli K C, Franco B E, Karaman I, Gaydosh D and Noebe R D 2013 Influence of crystallographic compatibility on residual strain of TiNi based shape memory alloys during thermo-mechanical cycling *Mater. Sci. Eng. A* 574 9–16

[42] Dagdelen F, Balci E, Qader I N, Ozen E, Kok M, Kanca M S, Abdullah S S and Mohammed S S 2020 Influence of the Nb content on the microstructure and phase transformation properties of NiTiNb shape memory alloys *JOM* 72 1664–72

[43] Wang X B, Verlinden B and Van Humbeeck J 2014 R-phase transformation in NiTi alloys *Mater. Sci. Technol. (United Kingdom)* 30 1517–29

[44] Ren X, Miura N, Zhang J, Otsuka K, Tanaka K, Koiwa M, Suzuki T, Chumlyakov Y I and Asai M 2001 A comparative study of elastic constants of Ti-Ni based alloys prior to martensitic transformation *Mater. Sci. Eng. A* 312 196–206

[45] Wang X, Verlinden B and Van Humbeeck J 2015 Effect of post-deformation annealing on the R-phase transformation temperatures in NiTi shape memory alloys *Intermetallics* 62 43–9